ISBN: 978-3-95450-247-9 ISSN: 2673-5490 doi: 10.18429/JACoW-IPAC2024-TUPG20

NUMERICAL OPTIMIZATION OF THE DIAMOND-II STORAGE RING OPTICS

N. Blaskovic Kraljevic*, H.-C. Chao, H. Ghasem, I.P.S. Martin, S. Preston,
Diamond Light Source, Oxfordshire, UK

Abstract

The design performance of the 3.5 GeV Diamond-II low-emittance electron storage ring has been studied as a function of the linear and nonlinear lattice tuning parameters. An alternative working point has been identified which optimizes the beam lifetime and the injection efficiency for off-axis injection. The simulations include misalignment and field strength errors, with the number of machine seeds tuned to achieve converging results whilst minimizing computational time. The optimization takes care to preserve the design beam emittance, energy spread, Twiss parameters and cell tunes. The results are presented for 2D parameter scans and exploring the null space of the chromaticity response matrix.

INTRODUCTION

In order to improve the beam lifetime and injection efficiency (IE), an investigation has been performed to identify potential alternative working points by adjusting the quadrupole and sextupole strengths of the Diamond-II storage ring. In this paper we present detailed tune and chromaticity scans, as well as explore the null space of the chromaticity response matrix, in which groups of sextupole strengths are modified to alter the nonlinear lattice whilst keeping the chromaticity unchanged.

SIMULATION

The Diamond-II storage ring [1] lattice in elegant [2] was used, including apertures for closed collimators and insertion devices. Random errors were applied to each of 5 machine seeds consisting of Δx, Δy transverse misalignment errors, roll errors and fractional strength errors (FSEs); the 'reduced' errors applied (Table 1) replicate the final, corrected machine performance after all optics corrections steps have been applied, without needing to conduct the lengthy and time-consuming commissioning procedure [1]. It was found that whilst there was variation seed-to-seed, averaging over 5 seeds produced reliable results. This was tested by studying 20 seeds and assigning them randomly to 4 groups containing 5 seeds each; averaging the results for each group gave consistent results across the 4 groups.

The simulation procedure consisted of the following steps:

1. Apply reduced errors
2. Trajectory correction with sextupoles off
3. Turn on sextupoles and add random, systematic and steering multipoles
4. Trajectory correction
5. Orbit correction
6. Tune correction
7. Chromaticity correction

Tune correction was performed in elegant using five families of quadrupoles located in dispersion-free regions at the ends of the standard and long straights (Q1N, Q2N, Q0L, Q1L and Q2L) to correct the horizontal and vertical tune to the desired values. Comparing the results to using only the quadrupole families in the standard straights (Q1N and Q2N) shows that the use of five quadrupole families allows the individual cell tunes to be better preserved (that is, maintaining the 24-cell pseudo-symmetry of the ring) on performing a tune correction, but does not affect the IE, Touschek lifetime (TL) or energy spread.

Similarly, chromaticity correction was performed using all three families of chromatic sextupoles (S2A, S3A and S4A) to correct the horizontal and vertical chromaticity.

The TL was calculated by computing the momentum aperture at the sextupoles after tracking a stored beam for 500 turns. The IE was evaluated by injecting a beam at a 4.5 mm offset and computing the fraction of particles successfully stored after 2048 turns. Note that, whilst the Diamond-II design calls for a 4mm off-axis injection, a larger offset was intentionally used in simulation to account for injected beam steering errors and enhance the losses.

TUNE AND CHROMATICITY SCANS

The horizontal and vertical tunes (ν_x and ν_y, respectively) were scanned in steps of 0.01 as shown in Fig. 1, by following the simulation procedure outlined in the previous section and updating the tune correction target in step 6. The plots show the clear effect of resonance lines, which in the case of the IE are shifted due to the tune shift with amplitude experienced by the off-axis injected beam.

The nominal tune point $(\nu_x, \nu_y) = (54.14, 20.24)$ returns a mean TL of 2.14 h and an IE of 96.4 %. A number of alternative working points have been identified at lower vertical

Table 1: Reduced Errors

Element	$\Delta x, \Delta y$ **(µm)**	**Roll (µrad)**	**FSE**
Dipole	15	100	1×10^{-4}
Antibend	15	100	1×10^{-3}
Quadrupole	15	100	1×10^{-3}
Sextupole	15	100	1×10^{-3}
Octupole	15	100	1×10^{-3}
BPM	10	20	–

* neven.blaskovic-kraljevic@diamond.ac.uk

ISBN: 978-3-95450-247-9 ISSN: 2673-5490 doi: 10.18429/JACoW-IPAC2024-TUPG20

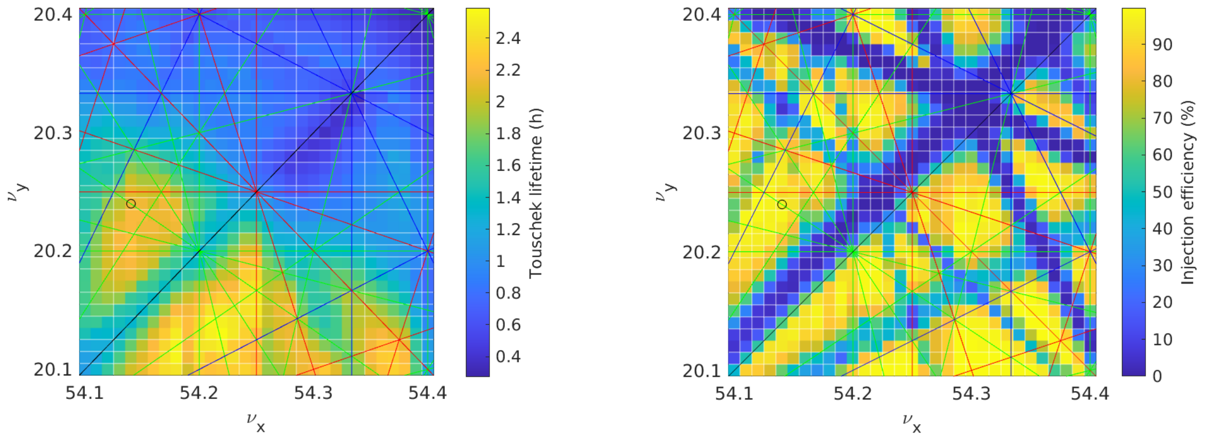

(a) TL (b) IE

Figure 1: Tune scan, averaging over 5 machine error seeds, with resonance lines overlayed. Nominal tune point shown by ∘.

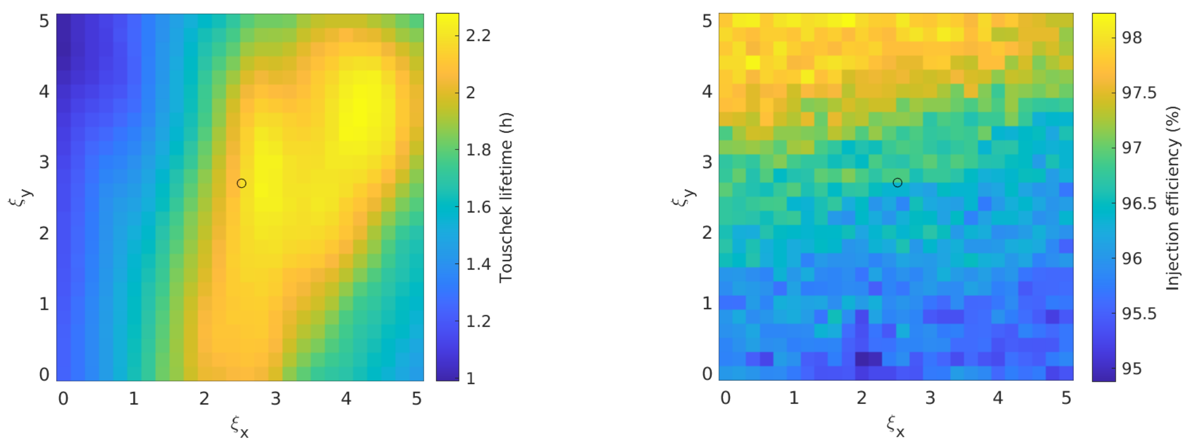

(a) TL (b) IE

Figure 2: Chromaticity scan, averaging over 5 machine error seeds. Nominal chromaticity point shown by ∘.

tunes (Table 2) that improve both TL and IE; however, approaching integer tunes amplifies the impact of dipole errors and quadrupole vibration on closed orbit distortions.

Similarly, the horizontal and vertical chromaticities (ξ_x and ξ_y, respectively) were scanned in steps of 0.2 as shown in Fig. 2, whilst keeping the tune at the nominal value (ν_x, ν_y) = (54.14, 20.24). Starting from the nominal chromaticity (ξ_x, ξ_y) = (2.52, 2.70), with a TL of 2.14 h, it can be seen that a higher TL can be achieved by increasing the chromaticity towards (ξ_x, ξ_y) = (4, 4). A peak TL of 2.28 h is obtained at the chromaticity set point (ξ_x, ξ_y) = (4.2, 3.8).

Table 2: Alternative Tune Working Points

ν_x	ν_y	**TL (h)**	**IE (%)**
54.14	20.24	2.14	96.4
54.21	20.16	2.25	97.6
54.23	20.11	2.42	97.2

A higher chromaticity would also help to increase instability thresholds, particularly during commissioning before the harmonic cavity is available. However, it has also been observed to reduce the efficacy of the transverse multi-bunch feedback, so would be less desirable during operations.

CHROMATICITY RESPONSE MATRIX

The Diamond-II storage ring consists of six families of sextupoles: three families of chromatic sextupoles (S2A, S3A and S4A) and three families of geometric sextupoles (S1X, S5X and S6X). As only two combinations of sextupoles (predominantly the chromatic sextupoles) are required to adjust ξ_x and ξ_y, we investigated varying groups of sextupoles occupying the null space of the chromaticity response matrix, that is, adjusting the sextupole strengths in combinations that preserve the nominal chromaticity [3].

A chromaticity response matrix R was constructed by calculating the effect of varying the sextupole K2 gradients on ξ_x and ξ_y:

ISBN: 978-3-95450-247-9 ISSN: 2673-5490 doi: 10.18429/JACoW-IPAC2024-TUPG20

$$\mathrm{R} = \begin{pmatrix} d\xi_x/d\mathrm{K2_{S1X}} & d\xi_y/d\mathrm{K2_{S1X}} \\ d\xi_x/d\mathrm{K2_{S2A}} & d\xi_y/d\mathrm{K2_{S2A}} \\ d\xi_x/d\mathrm{K2_{S3A}} & d\xi_y/d\mathrm{K2_{S3A}} \\ d\xi_x/d\mathrm{K2_{S4A}} & d\xi_y/d\mathrm{K2_{S4A}} \\ d\xi_x/d\mathrm{K2_{S5X}} & d\xi_y/d\mathrm{K2_{S5X}} \\ d\xi_x/d\mathrm{K2_{S6X}} & d\xi_y/d\mathrm{K2_{S6X}} \end{pmatrix},$$

and then decomposing it using singular value decomposition (SVD):

$$\mathrm{R} = \mathrm{USV^T}.$$

The six columns of the matrix U constitute the sextupole eigenvectors; each eigenvector U_i constitutes a 'knob' that can be added to the vector of nominal sextupole strengths to produce a new set of sextupole strengths:

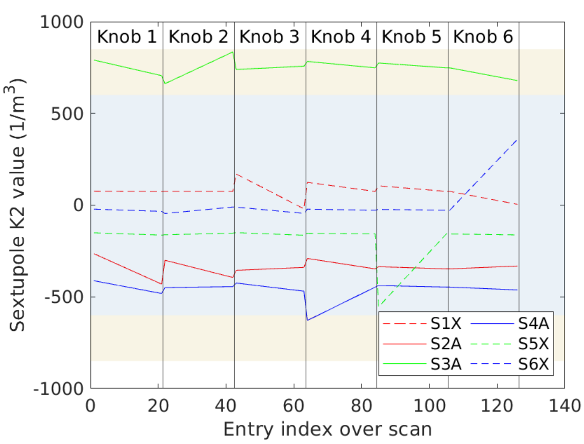

Figure 3: Sextupole strengths on sequentially scanning each of the six knobs. Full lines indicate chromatic sextupoles; dashed lines indicate geometric sextupoles. The inner blue shaded region indicates the power supply range for S1X, S2A, S5X and S6X; the outer yellow shaded region indicates the additional power supply range for S3A and S4A.

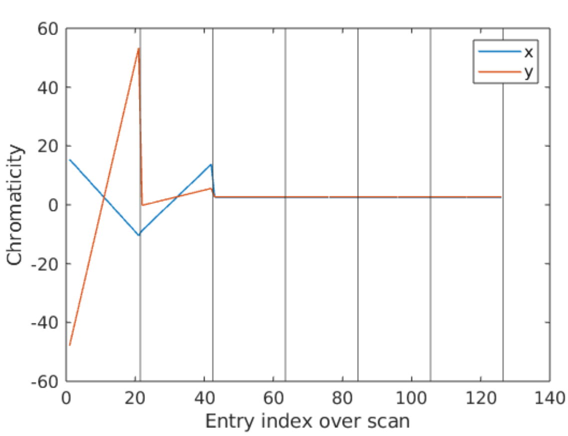

Figure 4: Horizontal and vertical chromaticities on sequentially scanning each of the six knobs as given in Fig. 3.

$$\begin{pmatrix} \mathrm{K2_{S1X}} \\ \mathrm{K2_{S2A}} \\ \mathrm{K2_{S3A}} \\ \mathrm{K2_{S4A}} \\ \mathrm{K2_{S5X}} \\ \mathrm{K2_{S6X}} \end{pmatrix}_{\mathrm{new}} = \begin{pmatrix} \mathrm{K2_{S1X}} \\ \mathrm{K2_{S2A}} \\ \mathrm{K2_{S3A}} \\ \mathrm{K2_{S4A}} \\ \mathrm{K2_{S5X}} \\ \mathrm{K2_{S6X}} \end{pmatrix}_{\mathrm{nominal}} + nU_i$$

where n is the knob strength for the given knob i.

Each of the six knobs was scanned sequentially, as shown in Fig. 3, leading to the chromaticity variation shown in Fig. 4. It was confirmed that the sextupole strengths are within the design power supply limits.

Knobs 1 and 2, which leave the geometric sextupoles almost unchanged, adjust the horizontal and vertical chromaticities. On the contrary, knobs 3 to 6 fully preserve the chromaticities at the initial, nominal values $(\xi_x, \xi_y) = (2.52, 2.70)$. It is knobs 3 to 6 that can be used to explore the null space of the chromaticity response matrix.

Figure 5 shows the TL on scanning the six knobs for an ideal machine without machine errors. The nominal TL (in the absence of errors) of 2.45 h can be improved to 3.06 h using knob 5 and 3.27 h using knob 6.

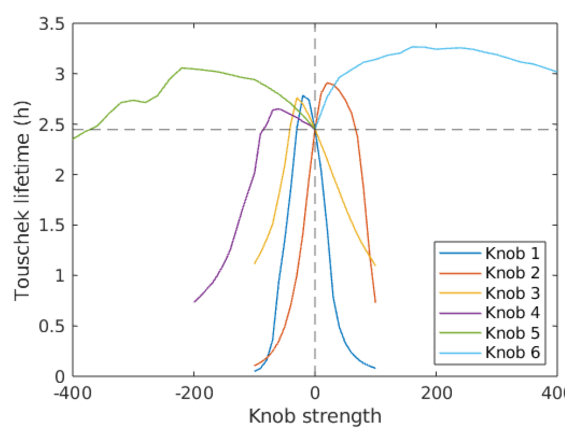

Figure 5: TL in the absence of machine errors on scanning the six knobs independently. The dashed lines indicate the nominal TL of 2.45 h (at knob strength = 0) in the absence of errors.

CONCLUSION

The TL and IE as a function of tune and chromaticity have been mapped out and alternative working points have been identified which could improve the Diamond-II storage ring's performance. In addition, the null space of the chromaticity response matrix has been explored by using sextupole strengths that preserve the nominal chromaticity but significantly improve the TL for an ideal machine. Further work, to include machine errors and the effect on IE, are necessary but the results are promising as they may allow an improvement in machine performance whilst preserving the storage ring's tune and chromaticity.

ISBN: 978-3-95450-247-9 ISSN: 2673-5490 doi: 10.18429/JACoW-IPAC2024-TUPG20

REFERENCES

[1] R.P. Walker *et al.*, Diamond-II Technical Design Report, Aug 2022. `https://www.diamond.ac.uk/Diamond-II.html`

[2] M. Borland, "elegant: A Flexible SDDS-Compliant Code for Accelerator Simulation," Advanced Photon Source LS-287, September 2000. `doi:10.2172/761286`

[3] Z. Martí, G. Benedetti, M. Carlà, and U. Iriso, "ALBA beam lifetime optimization using RCDS", in *Proc. IPAC'23*, Venice, Italy, May 2023, pp. 3101–3103. `doi:10.18429/JACoW-IPAC2023-WEPL002`